THE AMERICAN SOCIETY OF MECHANICAL ENGINEERS
345 E. 47th St., New York, N.Y. 10017

96-GT-253

IMPACT OF ROTOR WAKES ON STEADY-STATE AXIAL COMPRESSOR PERFORMANCE

P. Deregel and C. S. Tan
Gas Turbine Laboratory
Massachusetts Institute of Technology
Cambridge, MA 02139
USA

Abstract

This paper addresses the causal link first described by Smith between the unsteady flow induced by the rotor wakes and the compressor steady-state performance. As an initial step, inviscid flow in a compressor stage is examined. First of a kind numerical simulations are carried out to show that if the rotor wakes are mixed out after (as opposed to before) the stator passage, the time-averaged overall static pressure rise is increased and the mixing loss is reduced. An analytical model is also presented and shown to agree with the numerical results; the model is then used to examine the parametric trends associated with compressor design parameters.

Nomenclature

A - wake axial veloicy defect
a - velocity defect in quasi-one-dimensional wake
B - coefficient defining wake thickness
b - width of quasi-one-dimensional wake
c - chord
$E(x)$ - integer part of x
h - stator pitch normalised by axial stator chord
K - stator-to-rotor blade ratio
L - loss coefficient (normalised by inlet dynamic head)
P - pressure (normalised by inlet dynamic head)
Re - Reynolds number based on axial stator chord
RHS - right hand side
T - without subscript, denotes rotor wake passing period
T - with subscript, denotes traverse time for fluid element
t - time
U - velocity vector in the stator frame
u - axial component of U
V - scalar velocity given by $\sqrt{u^2+v^2}$
v - tangential component of U
W - velocity vector in the rotor frame
w - velocity within the wake in the rotor frame
x - axial coordinate
y - tangential coordinate
Z - (absolute) wake velocity defect
α - wake angle with respect to the y-axis
δ - wake width
$\delta\eta$ - change in efficiency
ϕ - flow coefficient
γ - angle between the wake and the steady (base) flow
Γ - circulation
ρ - density
θ - steady (base) flow angle with respect to the x-axis
ω - vorticity vector
Π - Pressure coefficient(normalised by inlet dynamic head)
Δ - change in
Δ_W - wake velocity defect (in Table III)

Subscripts

A - area and time-averaged
a - case a (unsteady)
adv - advection
b - case b (steady)
in - inlet
$isen$ - isentropic
M - mixed out values
out - outlet

Presented at the International Gas Turbine and Aeroengine Congress & Exhibition
Birmingham, UK — June 10-13, 1996

p - perturbation flow quantity
ps - pressure side
ref - reference values
ss - suction side
t - stagnation quantities
w - value in the wake
x - axial component
y - tangential component
∞ - far upstream from the stator

Superscripts

K - pertains to that associated with kinetic energy
P - pertains to that associated with pressure
$\overline{()}$ - average value

1 Introduction

Most of the current design methods in turbomachinery are primarily based on steady-state aerodynamics. It has been argued that further improvements in turbomachinery performance can be achieved if the influence of unsteady flows on time averaged performance can be quantitatively understood. In multistage axial compressors, two major sources of flow unsteadiness associated with blade relative motions are potential interaction between blade rows and wake-blade interaction. The latter can have an important influence on blade pressure distribution and resulting flow field development. However, it is still unclear if (and how) the presence of blade wakes modifies the steady-state compressor efficiency and pressure rise. Any mechanisms associated with wake-blade interaction that impact time-averaged performance of compressor blade-rows would be of engineering interest.

From a designer point of view, particularly when dealing with the effects of unsteady flows, effort should be focussed on answering well-defined fluid dynamic questions (Greitzer, et al.,1995) (Munk,1981). *A specific fluid dynamic question of practical relevance to be asked and resolved would be: are the time-averaged overall static pressure rise and mixing loss modified if the rotor wakes are mixed out after (case a) as opposed to before (case b) the stator passage ?* This paper is aimed at addressing this question and it is organised as follows.

Experimental results and simple analyses are first presented in Section (2) in order to motivate the subject matter before stating the overall technical objective and making hypotheses on the flow in Section (3). With these hypotheses, the question is first addressed in Section (4) by examining the computed results from inviscid unsteady flow simulations involving rotor wakes interacting with a stator blade row. Numerical results (from the inviscid simulations) are summarized and given a qualitative explanation in Section (5). The physical mechanisms thought to be responsible for the enhanced stator performance characteristics in case a as compared to that in case b are used to develop a flow model in Section (6). The model is first assessed against the numerical results in Section (7); this is then followed by its application in Section (8) to examine the parametric dependence of stator performance characteristics on compressor design parameters such as blade loading, flow coefficient and axial rotor-stator gaps. These trends are physically explained and briefly discussed in specific flow situations of interest. Finally the key results and conclusions are given in Section (9).

2 Background and Motivation

In this section experimental results and simple analyses are presented to motivate the investigation of time-averaged impact of wake-blade interactions on performance.

2.1 Experimental Results

Multistage axial compressors have experimentally been shown to exhibit both a higher pressure rise and a higher efficiency when the axial gap between the blade rows is reduced. This is illustrated in Fig. 1 (Smith, 1970) where data from two tests on a three-stage low speed research compressor are shown. For the first test the axial spacing was 7% of chord, and for the second one it was 37% of chord. There is a one or two percent increase in efficiency and a two to four percent increase in static pressure rise for compressor with reduced axial rotor-stator gap. Similar trends were also experimentally found by Mikolajczak (1977).

In these two studies, the data do not directly show that the enhancements are due to unsteady flow. Smith (1966) suggests that this increase in performance for compressor with a reduced gap is explained by a stronger flow unsteadiness in the blade passage than for that with a large gap (where the wakes can probably be assumed to be mixed out before entering the stator passage). Smith(1966, 1993) also provides the following plausible explanation (see illustration in Fig. 2) for the increase in efficiency when the axial gap is reduced:-

If we assume that the flow is inviscid and the density constant, then by Kelvin's theorem, the circulation around the contour C remains constant as the wake is convected through the passage. Therefore the velocity difference between the wake and the free stream decreases in inverse proportion to the length of the wake. This means that if the wake were mixed out at the exit (i.e. section 2 in Fig. 2), the associated loss could indeed be less than if the wake were mixed out before entering the passage (i.e. section 1 in Fig. 2).

2.2 Mixing

The mixing process (schematically described in Fig. 3a) is characterized by the action of viscous forces on flow nonuniformities

entering at section 1, leading to an eventual uniform state at section 2. The effects of mixing depend on both the flow nonuniformities at section 1 and what happens to the flow between section 1 and 2. Throughout this study, we shall assume that mixing occurs at constant area. In physical terms, the mixing process leads to a reduction in axial momentum flux, which in turn produces an increase in pressure rise. The irreversible mixing process also generates loss, i.e. the increase of specific entropy that can be approximated by the reduction of mass averaged total pressure (Denton,1993). This loss is measured in terms of a *loss coefficient* that is equal to minus the time-averaged creation of specific entropy associated with mixing and it is expressed as a percentage of the inlet dynamic head ($\rho\frac{U_{in}^2}{2}$) [1] .

To obtain an idea of the parametric dependence of mixing, we can examine the simple flow situation of a quasi-one-dimensional wake shown in Fig. 3b. It can be shown that [2] both the pressure rise and the loss associated with mixing scale *quadratically* with the velocity defect [3] in the wake and linearly with its width. The velocity nonuniformity in the case of stator passage, though not a simple one-dimensional wake, follows a relatively similar scaling. If the wakes are effectively stretched in the stator passage before being mixed out, we can indeed expect a diminution of mixing loss as Smith had originally proposed.

2.3 Pressure Rise

The incompressible Navier-Stokes equations, written as :

$$\begin{cases} \frac{\partial \mathbf{U}}{\partial t} + \mathbf{U}\cdot\nabla\mathbf{U} = -\nabla P + \frac{1}{Re}\nabla\times\omega \\ or \\ \frac{\partial \mathbf{U}}{\partial t} + \nabla\frac{U^2}{2} - \mathbf{U}\times(\nabla\times\mathbf{U}) = -\nabla P + \frac{1}{Re}\nabla\times\omega \\ \nabla\cdot\mathbf{U} = 0 \end{cases} \quad (1)$$

can be used to derive an expression for the pressure rise. The flow variables are made dimensionless using the axial stator blade chord c_x, the density ρ and the axial velocity u_∞ far upstream of the stator.

The pressure rise is defined as the difference in time and area averaged pressure between the inlet and the outlet. By multiplying the Navier-Stokes equation by the axial unit vector i, applying Gauss theorem to the region S shown in Fig. 2 and integrating over a time period, we obtain :

$$\int_t^{t+T}\left(\int_{outlet} P - \int_{inlet} P\right)dydt = -\int_t^{t+T}\int_{ss+ps} P_t\,\mathbf{i}\cdot\mathbf{n}dxdt$$

$$-\int_t^{t+T}\left(\int_{outlet} - \int_{inlet}\right)\frac{U^2}{2}dydt + \int_t^{t+T}\iint_S \mathbf{i}\cdot\mathbf{U}\times(\omega)dxdydt - \int_t^{t+T}\iint_S \mathbf{i}\cdot\frac{1}{Re}\nabla\times\omega dxdydt \quad (2)$$

The four terms on the RHS of Eq. (2) correspond to a total pressure drag, a transfer from kinetic energy to pressure rise, a vortex force and a viscous term (which vanishes for an inviscid flow) respectively. Each of these contributions [4] to the passage pressure rise can potentially be modified by the presence of wakes in the stator passage; they thus provide plausible means for explaining any change in the time-averaged pressure rise associated with unsteady wake-blade interactions.

With the above (i.e. experimental observations, Smith's explanation, loss associated with mixing-out of flow non-uniformities and physical processes in establishing the pressure rise across a blade-row) as background, we will propose to examine the change in time-averaged pressure rise and mixing loss (associated with wake-blade interactions) based on the approach to be delineated in the next section.

3 Overall Technical Objectives and Approach

In this section the overall goal is stated; the approach taken to accomplish the state goal is then described.

3.1 Fluid Dynamic Questions to be Addressed

The overall goal is to address the following specific fluid dynamic questions :

- 1) What is the (time-averaged) mixing loss if the flow is mixed out at section 1 or at section 2 in Fig. 2 ?
- 2) What is the (time-averaged) difference in passage pressure rise if the flow is :
  - a) unsteady (isentropic) with wakes in the passage and then mixed out at section 2
  - b) Mixed out at section 1 and downstream of which the flow is isentropic

[1] As incompressible flow is assumed, ρ can be taken as unity

[2] keeping first order terms in $\frac{a}{b}$ and $\frac{b}{h}$

[3] relative to the free stream velocity

[4] As stated in Section (1), the focus of the present work is on inviscid flow so that we need not be concerned with the contribution from term 4 on the RHS of Eq. (2)

The above question will be examined for a flow situation that can be well approximated as inviscid, incompressible and two dimensional. Simulations are thus carried out with a time accurate two-dimensional inviscid incompressible code [5] where the incoming rotor wakes are modeled as a moving stator inlet velocity distortion. These simulations can be viewed as clean and simple numerical experiments devoid of effects associated with stator blade boundary layer (Valkov, 1992 and 1995) and flow three-dimensionality (Graf, 1996) (Valkov, 1996). As such these computed results can be contrasted with those from unsteady two-dimensional viscous simulations (Valkov, 1996) and unsteady three-dimensional simulations (Graf, 1996) (Valkov, 1996) for assessing the role, if any, of wake-blade boundary layer interactions and flow three-dimensionality on time-averaged performance (i.e. numerical experiments ought to be implemented at different levels of physical approximations to unsteady wake-blade interactions for sorting out specific cause-and-effect on time-averaged performance; the present work can thus be viewed as a step in this direction).

Such a flow situation would allow one to establish a causal link between the unsteady flow induced by the rotor wakes in the stator passage and its time-averaged performance characteristics without undue complexities.

3.2 Numerical Approach

Numerical simulations are to be carried out to answer the fluid dynamic questions stated above. To do so, the governing Eq. (1) [6] are solved by using a time splitting scheme (Orszag and Kells, 1980) for temporal discretization and a spectral element method for spatial discretization so that any resulting numerical dissipation can be kept minimal. The computational domain is the region S as defined in Fig. 2 [7], at the inlet of which the wakes (mixed out in case b) are simulated by a velocity distortions (see Appendix A for a description of the wake model). In order to somehow span the design domain, numerical simulations are carried out for both a stator of Eppler design (Eppler, 1990) with a pressure rise coefficient of 0.2 and a stator of E^3 design (Wisler, 1977 and 1981) that produces a pressure rise coefficient of 0.5. The latter is representative of that used in modern compressors. For the two blade geometries, the pitch (0.6 of axial stator chord) and the flow coefficient (0.5) are kept the same (a solidity of unity would be more representative rather than the value used here; its choice does not in any way impact the examination of technical questions posed in Section (3.1)).

For a given set of wake parameters (velocity defect and width) that are representative of experimental values (Table IV in Appendix A), two calculations are implemented:

- A calculation (case a) where the wakes are simulated by a periodic inlet velocity distortion; here we shall examine the (time-averaged) mixing loss and the (time-averaged) pressure rise in the passage as a function of axial location at which the flow is assumed to have mixed out .

- A calculation (case b) where the (steady-state) inlet conditions reproduces the *time-averaged* mass flow and tangential momentum of case a; this essentially yields the steady state pressure rise and the loss due to mixing out of wakes at the inlet (the increase in static pressure rise resulting from the mixing of the wakes at the inlet (see Section (2.2)) will be taken into account in Section (7)).

In what follows, we present and interrogate these numerical results in the context of questions posed in Section (3.1).

4 Numerical Results

Our primary focus in this Section is to determine how the mixing loss and the difference in pressure rise between the unsteady and the steady flow situations (i.e. case a and b respectively) varies with the axial location at which the flow is mixed out. The computed results will be used to show that the mixing loss is reduced if mixing occurs after as opposed to before the stator passage and that the isentropic presssure rise is higher in the unsteady flow situation.

4.1 Flowfields

For the two geometries, the disturbance flows are obtained by subtracting the steady flow (case b) from the unsteady flow (case a at a given time). In Fig. 4 and 5, the vorticity contours and the velocity vectors for the disturbance flows are shown for the Eppler and the E^3 geometry. As shown in Fig. 4 and 5, each wake [8] is composed of two vortex sheets of opposite sign. It is convected by the freestream flow (which turns and stretches it).

[5] The Kutta condition has been enforced numerically to ensure that there be no pressure jump at the trailing edge; the pressure distribution from the inviscid solution is in agreement with that from the Navier-Stokes calculation. As the use of Kutta condition in inviscid flow reflects the role of non-zero viscosity in setting up the correct blade circulation and hence the pressure distribution, the agreement in static pressure between the inviscid and Navier-Stokes solution indicates the consistent imposition of Kutta condition here. Alternatively the numerical viscosity present in the inviscid solution procedure can prevent the formation of a singularity at the blade trailing edge (i.e. infinite velocity at sharp trailing edge) and hence indirectly allows the Kutta condition to be satisfied

[6] For flow with inviscid assumption, one need not be concerned with the viscous term and therefore non-slip condition is not imposed on blade surfaces.

[7] S is divided into 1300 spectral elements, each of them having $7 \times 7 = 49$ points (7^{th} order method) at the inlet of which wakes (mixed out in case b) are simulated by inlet velocity distortions. Simulations were run with a times step of 5×10^{-4} s (convective time).

[8] The wake characteristics are summarized in Table IV at the end of Appendix A

4.2 Mixing Loss

The *time-averaged* mixing loss as a function of the x-location (at which the unsteady flow is assumed to have been mixed out) is shown in Fig. 6. In the two cases (Eppler and E^3 blade design), results show that the loss associated with the mixing is reduced if it occurs at the exit of the stator passage (as opposed to the inlet). At the inlet, the mixing loss coefficient [9] is approximately the same (0.9%) for Eppler and E^3 blade design; however mixing loss is reduced further in the case of the E^3 blade design, down to 0.15% at the outlet as compared to 0.3% for the Eppler.

4.3 Pressure Rise

The control volume analysis of Section (2.3) has shown that there are three terms that could potentially contribute to a difference in (time-averaged) pressure rise between the steady and the unsteady case. The change in total pressure drag is numerically found to be negligible (less than 0.1% [10]). The vortex force lead to a diminution of pressure rise of about half a percent. Its effect (confined on the suction side) is due to the presence of a street of negative vortices created when a wake intercepts with the leading edge [11] (For the viscous flow situations, positive vortices can be expected to appear between the blade and the negative vortices (Valkov, 1992, 1995), with the result that the net contribution is negligibly small (Valkov, 1996)). For this reason, the influence of vortex force (which appear as a spurious effect here) is not taken into account.

The difference in pressure rise between the unsteady and the steady case is plotted as a function of the axial location in Fig. 7. This shows a (time-averaged) passage pressure rise premium in the unsteady case (a) of about 1.5% of inlet dynamic head. This premium is slightly larger and attained earlier for the E^3 than for the Eppler blade design.

5 Summary and Further Physical Interpretation of Numerical Results

5.1 Mixing Loss

The numerical results of Section (4) clearly show a reduction in mixing loss if mixing out of flow non-uniformities (due to rotor wakes) were to occur at the outlet, as opposed to at the inlet. The wakes are stretched in the passage leading to a reduction of the velocity defect in the wakes at the outlet relative to that at the inlet; this is in line with the explanation originally put forward by Smith (1966, 1993) . The present numerical results indicate that the reduction in mixing loss scales with the diminution of wake velocity defect (from inlet to outlet) in a manner slightly more than the quadratic dependence.

Calculations for the case of Eppler blade (with wake velocity defect Z taken as 0.27 and 0.54, and with corresponding wake width δ taken as 0.32 and 0.16) have been implemented and the results show that the *inlet* mixing loss does *approximately* scale quadratically with the wake velocity defect and linearly with the wake width, in agreement with the results of a simple control volume analysis presented in Section (2.2).

5.2 Pressure Rise

Numerical results presented in Section (4.3) show a higher time-averaged pressure rise in case a of unsteady flow relative to case b of steady flow; this can be attributed to a larger reduction of the (time- and area-averaged) kinetic energy in the passage [12] . At the inlet of the Eppler blade passage, the kinetic energy in the wake is the same as the freestream value, but as the wake is convected through the passage, a kinetic energy defect appears in the wake that will in turn lead to a higher passage pressure rise. In contrast, at the inlet of the E^3 blade passage, there is an excess of kinetic energy in the wake relative to the freestream value. As the wake is convected through the [13]

passage, this excess first disappears before developing into a kinetic energy defect in the wake within the second half of the passage. This effect can be explained by the change of velocity triangle from the inlet to the outlet. The relatively larger transfer of kinetic energy in the unsteady case leads to a larger pressure rise [14].

5.3 Turning of the Wake

Numerical results of Fig. 4 and 5 show that the wakes, as they proceed from the inlet to the outlet, turn counter-clockwise by 5 degrees in the Eppler blade passage and clockwise by 4 degrees in the E^3 blade passage [15] . There are two physical effects that tend to turn the wakes in opposite directions. The first is a "diffuser effect"

[9] creation of specific entropy expressed as a percentage of the inlet dynamic head

[10] All the results regarding pressure rise are given as a percentage of the inlet dynamic head

[11] This effect is relatively more pronounced in the case of Eppler blade as it has a sharper leading edge; this spurious effect is associated with high flow gradient in the immediate leading edge region where numerical dissipation can be non-negligible; however its contribution is negligibly small compared to the overall change in time-averaged pressure rise

[12] The kinetic energy in the wake changes with axial position as the local velocity triangle evolves axially through the blade passage; it can be less than, the same as, or greater than the freestream value.

[13] where the loading is defined as the static pressure rise divided by the inlet dynamic head.

[14] Note that in the steady case, the flow can perceive a larger reduction of the kinetic energy than the unsteady case but the effect of the apparition of a relatively large kinetic energy defect in the wake is preponderant.

[15] with respect to a fixed frame

illustrated in Fig. 8a : a decrease in velocity in the axial direction x implies that the farther end of the wake is convected slower than the other section. As a result, the wake tends to turn clockwise; the strength of this first effect depends on the pressure gradient in the x-direction. The second is a "circulation effect" (illustrated in Fig. 8b): at a given axial location the flow velocity is greater on the suction surface than on the presure surface, so that it induces a rotation counter-clockwise. For example, at the inlet of the E^3 passage (in Fig. 5), the wakes indeed turn counter-clockwise due to a relatively strong circulation around the leading edge. It is rather interesting to note that these two competing effects from which the actual turning results equilibrate before the end of the passage for these two blade designs; as a consequence, the wake angle [16] at the outlet has a weak dependence on the inlet wake angle.

6 Development of An Analytical Model

We have used the numerical results to develop a physical explanation for the observed improvement in time-averaged stator performance characteristics. To complement the computations, we will propose an analytical model based on control volume approach and kinematics of wake-blade interaction. The model is then used in Section 8 to examine the parametric trends of (time-average) performance associated with some of the compressor design parameters.

6.1 Integral Forms

The control volume analyses of Appendix B provide integral forms for both mixing loss at the inlet and at the outlet, as well as the difference in static pressure rise between the unsteady and the steady flow situation. The expression for the loss coefficient contains four terms: the first two depend directly on velocities while the third can also be expressed in terms of velocities using the axial momentum equation; the computed results (for Eppler and E^3 blading used here) indicate that the fourth term is negligibly small. Thus it may be deduced that only a *kinematic* description of the flow at the inlet and at the outlet can be used to determine the changes in pressure rise and loss associated with wake-blade interactions; specifically, only the difference between the flow kinematic characteristics at these two locations obtained before and after mixing (in the unsteady case) is needed. These observations and inferences form the guideline for developing a model based on an approximate kinematic description of wake-blade interaction.

[16] The wake angle is defined as the angle between the wake and the vertical axis y

6.2 An Approximate Kinematic Description of Flow

As stated, only those aspects of the flow which affect the difference between the flow before and after mixing (both at the inlet and the outlet) are of interest. We shall therefore focus on these specific aspects of the flow that can significantly alter this difference. The unsteady flow can be taken as the superposition of a (steady) flow [17] and an unsteady disturbance flow associated with the wake passage. The flow features that essentially constitute the key ingredients for the analytical model are described in Appendix C.

The inlet disturbance velocity field is given in Eq. 6 of Appendix A. For the outlet disturbance flow, we must first determine the wake angle α_{outlet}, the extent of the wake stretching s_{outlet} between the inlet and the outlet of the stator passage as well as the extent of the wake advection. α_{outlet} and s_{outlet} are determined from geometrical constructions presented in Appendix C. In order to predict how much the wakes are self-advected, we assumed the self-advection (constant) velocity to be half of the wake average [18] velocity defect.

6.3 Integrated Expressions

The above kinematic description of the flow at the inlet and the outlet can be substituted for u and v in the integral expressions given in Appendix B. Since the velocity profiles are Gaussian, analytical results can be obtained.

6.4 Summary : inputs and outputs to/from model

The inputs to the model are : the inlet wake coefficients (see Appendix A), the inlet and outlet steady flow angles (θ_{inlet} and θ_{outlet}), the difference in traverse time for a fluid element along pressure and suction side, the stator pitch-to-chord ratio and the flow coefficient.

The outputs from the model are : the difference in time-averaged passage pressure rise between the unsteady and the steady flow situation, the inlet and the outlet mixing loss, and the associated time-averaged static pressure rise (see Section 2.2) in the unsteady flow situation.

The integral expressions given in Appendix B can be used to compute the change in performance of a stator interacting with upstream moving wakes; they will be used in Section 8 to examine the parametric trends.

[17] In using the analytical model for obtaining mixing loss and change in pressure rise between case (a) and (b), the effect due to velocity variation across the blade passage is negligibly small for the cases examined here

[18] the average wake velocity defect is defined as its average value between the inlet and the outlet

7 An Assessment of Analytical Model Against Numerical Results

7.1 Turning and Stretching of Wakes in Blade Passage

For Eppler and E^3 blading with a flow coefficient of 0.5, the turning of the wakes can reasonably be predicted. The geometrical stretching s_{geom} (i.e. of how much a contour similar to C in Fig. 2 is stretched between the inlet and the outlet) can also be determined (1.4 and 1.8 for the Eppler and the E^3 blade geometry respectively).

7.2 Mixing loss

The comparison between the results obtained for mixing loss coefficients based on numerical simulations and the model are summarized in Table I.

Table I : Mixing Loss Coefficient in Case a and b

Blading	Mixing out at inlet		Mixing out at outlet	
	simulation	model	simulation	model
Eppler :	0.9	0.88	0.30	0.32
E^3	0.9	0.83	0.15	0.16

These results indicate that mixing loss at the inlet and the outlet can be predicted with less than a 10% error.

7.3 Pressure rise

The computed results for pressure rise are compared against those from the model in Table II.

Table II : Pressure Rise Coefficient: Case a vs b

Blading	Simulation	Model		
	$\Pi_{\Delta Pisen}$	$\Pi_{\Delta Pisen}$	$\Pi_{\Delta PM}$	
			inlet	outlet
Eppler	1.3	1.11	0.45	0.25
E^3	1.6	1.51	0.64	.12

For the Eppler and the E^3 blading, the model underpredicts the premium in isentropic pressure rise of 15% and 6%, respectively.

Simulations (not shown here) have been carried out for the Eppler and the E^3 blading with different wake parameters (including velocity defects of up to 50%). They show an underprediction of $\Delta P_{isentropic}$ of $5-15\%$. These simulations also show that the inlet and the outlet mixing loss are predicted by the model within less than a 10% error. These results not only complement the numerical study, but also imply that the model can be used to examine parametric trends of interest.

The *overall* premium in (time-averaged) pressure rise is :

$$\Pi_{\Delta Poverall} = \Pi_{\Delta Pisentropic} + \Pi_{\Delta Pmixing}(outlet) - \Pi_{\Delta Pmixing}(inlet) \quad (3)$$

As shown in Table II the pressure rise associated with mixing is larger at the inlet than at the outlet, which therefore tend to reduce the overall pressure rise (of 0.20% for the Eppler and 0.52% for the E^3 case). These numbers should be compared to the respective isentropic pressure rise of 1.3% and 1.6%, respectively. In this respect, the static pressure rise increase associated with mixing is not quite negligible and will be taken into account in the following Section.

8 Parameter Trends

The analytical model of Section (7) can be used to examine the parametric trends of interest, and can also be compared with available experimental data for assessment purpose. In this Section we apply it to explore the influence of inlet flow angle, flow coefficient and axial rotor-stator gap on the performance characteristics of stator blade rows.

8.1 Effect of a Change in Blade Loading

When the blade loading is increased, wakes are stretched further which therefore leads to a larger relative diminution in mixing loss between the inlet and the outlet. However for constant axial velocity defect and flow coefficient, the absolute wake velocity defect decreases with inlet flow angle(and hence stator blade loading). As the results of Fig. 10 (for a flow coefficient of 0.5 but with wakes that have a constant axial velocity defect of 0.15 and with the variation in inlet flow angle determined based on values used for Eppler and E^3 blade) show, both the mixing loss and the premium in pressure rise coefficient decrease with an increase of blade loading. This effect is magnified when the results are expressed in term of changes in efficiency and relative pressure rise [19].

8.2 Variation of Flow Coefficient for E^3 Blading

In Fig. 11, we plot the difference[20] between the inlet and the outlet mixing loss and the pressure rise premium coefficient as a function of the flow coefficient ϕ for the E^3 passage. In doing so, we assumed that both the passage loading and the wake axial velocity defect do not vary with the flow coefficient ϕ. The mixing loss and the pressure rise increase when the flow coefficicent is reduced. As the axial wake velocity defect is kept constant, the absolute wake velocity defect thus increases with a reduction of flow coefficient. In addition, the stator inlet velocity angle θ is increased and the

[19] The change in efficiency associated with mixing and the relative increase in pressure rise are obtained by dividing the mixing loss and the premium in pressure rise coefficient by blade passage loading.

[20] in absolute value.

wake angle α is reduced which substantially increases the angle γ between the freestream velocity and the wake (see Fig. 9). The latter effect leads [21] to a relatively larger wake kinetic energy. This explains the increase in pressure rise premium when ϕ is reduced.

8.3 Results based on Experimental Data

In Table III, mixing loss and pressure rise coefficients are calculated, based on experimental data obtained by Silkowsky for two different flow coefficients (Silkowsky, 1995). The corresponding changes in wake charactersitics, inlet flow angle θ_{inlet} and blade row solidity are appropriately accounted for in the model.

Table III : Mixing Loss and Pressure Rise Premium

ϕ	θ_{in}	$\Delta w/u$	δ	ΔP	$\bar{L}_{in}$	$\bar{L}_{out}$	$\delta\eta$
0.42	44	18 %	0.31	0.9	0.8	0.2	1.2 %
0.38	49	33 %	0.19	1.7	1.6	0.4	2.4 %

A flow coefficent of 0.42 is near the design point, while one of 0.38 is close to stall. The gain in (total pressure) efficiency (apparently due to mixing) if the flow is mixed out at the exit is given in the last column. Table III provides a good quantitative estimate of the impact of the unsteady flow on steady-state performance (which is more pronounced at the lower flow coefficient).

8.4 Role of Unsteadiness on Enhancement in Time-averaged Stator Performance Characteristics

Results from numerical simulations showed that the *time averaged* tangential momentum flux at the passage outlet is the same in the unsteady and the steady case (i.e. case a and b). If this tangential momentum flux were constant with time in case a and since the axial velocity u_{Ma} is constant with time, the mixed out tangential velocity v_{Ma} would also be invariant with time. Thus, the only way that the loss generated within the passage can appear is in the form of a change in static pressure between case a and b. The difference in both passage pressure rise and mixing loss between case a and b as a function of the inlet flow angle is plotted in Fig. 10[22]. The difference between these two curves (due to unsteadiness) is seen to decrease with blade loading. This result appears to indicate that the effect of unsteadiness on performance enhancement would diminish as the stator loading is increased.

8.5 Effect of a Change in Axial Rotor-Stator Gap

We have assumed that for reduced axial rotor-stator gap, wakes are present at the stator inlet while for larger axial gap, the wakes are fully mixed out before entering the stator passage. To assess the goodness of this assumption, we examined the experimental results (Stauter,1991) from a two stage axial compressor (LSRR2). Results based on the use of experimentally-determined wake characteristics at various axial locations from the rotor are used to calculate the passage mixing loss and the pressure rise enhancement; these are shown in Fig. 12. Note the change in performance as the axial gap is increased as well as the values that represent changes in efficiency of the order of one percent and *relative* changes in pressure rise of up to 4 percent.

9 Summary and Conclusions

The overall problem addressed was the time-averaged impact of unsteady flow induced by rotor wakes on the stator steady-state performance; this was motivated by Smith's experimental observations (1970) in multistage compressors that show a higher pressure rise and a higher efficiency when the axial gap between blade rows is reduced. In the light of these observations, numerical simulations and an analytical model have been implemented to determine if the time-averaged overall pressure rise and mixing loss are modified for flow situations where the rotor wakes are mixed out after (case a) as opposed to before (case b) the stator passage. It has been shown both numerically and analytically that in the unsteady case a as opposed to the steady case b:

- mixing loss is significantly reduced, primarily due to the stretching of the wakes in the passage.
- the overall pressure rise is larger due to a larger reduction of the (time- and area-averaged) kinetic energy between the inlet and the outlet of the passage.

These phenomena [23] imply an increase in both efficiency and pressure rise[24] of the order of one or two percent (based on wake characteristics from experimental data in geometries representative of modern compressors). These values [25] are of the same order of magnitude as the gain measured by Smith for the reduced versus large axial gap. Parametric studies have been carried out to demonstrate a larger gain (especially in pressure rise) when the flow coefficient is reduced, which also agrees with Smith's experimental results.

10 Acknoledgment

This work is supported by NASA grant No 3-1679 with Dr. John Adamczyk as technical monitor and by SNECMA with Mr. Vin-

[21] Note that, according to Section (5.4), the outlet wake angle γ has a weak dependence on its value at the inlet

[22] The axial wake characteristics are kept constant

[23] Note that these phenomena are present all across the passage and that therefnre they would be present in viscous flow situations.

[24] normalized by the stator inlet dynamic head.

[25] that can become substantially higher in low flow coefficient HP compressors.

cent Garnier as technical monitor. The authors are grateful to Mr. Theodore Valkov for his help and constructive inputs during the course of this work, and to Professor Edward M. Greitzer for posing the problem in the first place as well as for his many critical but valuable suggestions and comments during the course of this work. The authors would also like to thank the reviewers for offering critical comments which are instrumental in improving the organisation and quality of the manuscript. The authors would also like to acknowledge the help of Ms. D. Park and Mr. D. Tew in the preparation of figures.

11 References

Denton, J.D. 1993, "Loss Mechanisms in Turbomachines", ASME *Journal of Turbomachinary, 115, pp 621-656*

Eppler, E., 1990. Airfoil Design Data. Spinger-Verlag.

Graf, M., 1996, Private Comunication.

Greitzer, E. M., Tan, C.S., Wisler, D.C., Adamczyk,J.J., Stazisar,A.J. 1994, "Unsteady Flow in Turbomachiones : Where's the Beef ?" ASME 1994 *AD-Vol. 40, Unsteady Flows in Aeropropulsion*

Mikolajczak, A.A., 1977, "The Practical Importance of Unsteady Flow", in AGARD CP-177, *Unsteady Phenomena in Turbomachinary.*

Munk, M, 1981, "My Early Aerodynamic Research - Thoughts and Memories", *Annual Review of Fluid Mechanics, Vol. 13.*

Orszag, S., Kells, L., 1980, "Transition in Plane Poiseuille and Plane Couette Flow", *Journal of Fluid Mechanics, Vol. 96*

Silkowsky, P., 1995, "Measurements of Rotor Stalling in a Matched and a Mismatched Multistage Compressor", MIT GTL report # 221.

Smith, L. H., 1966, "Wake Dispersion in Turbomachines", ASME Transactions, *J. Basic Engineering, Series D, No. 3, pp. 688-690*

Smith, L.H., 1970, "Casing Boundary Layers in Multistage Axial Flow Compressors" in *Flow Research on blading, edited by L.S. Dzung, Elsevier Publishing company, Amsterdam*

Smith, L.H., 1993, "Wake Ingestion Propulsion Benefits", *Journal of Propulsion and Power, Vol. 9, No. 1.*

Stauter, R.C., Dring, R.P, Carta, F.O., 1991, "Temporally and Spatially Resolved Flow in a Two-Stage Axial compressor: Part I - Experiment", ASME Journal of Turbomachinery, 113(2), pg. 219 - 226.

Wisler, D. C., 1977, "Core Compressor Exit Stage Study: Voloume 1 - Blading Design," NASA CR-135391

Wisler, D. C., 1981, "Core Compressor Exit Stage Study: Volume 4 - Data and Performance Report for the Best Stage Configuration," NASA CR - 165357

Valkov, T., 1992, "Control of the Unsteady Flow in a Stator Blade Row Interacting with Upstream Moving Wakes," MS Thesis, Department of Aero. and Astro., May, 1992.

Valkov, T., 1995, "Control of the Unsteady Flow in a Stator Blade Row Interacting with Upstream Moving Wakes," ASME *J. of Turbomachinery, Vol. 117, pg. 97 - 105*

Valkov, T., 1996, Private Communications

Appendices

A Wake Model

The wakes are modeled as moving velocity distortions; the velocity distortion is assumed to have a Gaussian profile. The wake velocity profile in the *rotor* frame can be written as (Valkov, 1992, 1995):

$$\frac{w(y_w)}{W} = 1 - Ae^{-By_w^2} \tag{4}$$

where y_w is the distance from the center of the wake, A the maximum *axial velocity defect* in the wake[26] and B represents the thickness of the wake. The width of the wake δ is given in term of the distance between the locations where the axial velocity is equal to 99 percent of the free-stream value: i.e.

$$\delta = 2\sqrt{\frac{\ln 100A}{B}} \tag{5}$$

The wake velocity defect in the stator frame can be written as a function of y, t, the wake angle α and the maximum *absolute velocity defect* in the wake [27] :

$$\left\{ \begin{array}{c} u_w(y,t) \\ v_w(y,t) \end{array} \right\} = \left\{ \begin{array}{c} -Zf(y,t)sin(\alpha) \\ Zf(y,t)cos(\alpha) \end{array} \right\} \tag{6}$$

where at the inlet :

$$\left\{ \begin{array}{l} \alpha_{inlet} = \tan^{-1}\left(\frac{u_{inlet}}{\frac{u_{ref}}{\phi} - u_{inlet}tan\theta_{inlet}} \right) \\ Z = A\sqrt{1 + \left(\frac{\frac{u_{ref}}{\phi} - u_{inlet}tan\theta_{inlet}}{u_{inlet}} \right)^2} \end{array} \right. \tag{7}$$

The function $f(y,t)$ can be expressed as the sum of two moving overlapped Gaussian disturbances (Valkov 1992, 1995)

$$f(y,t) = \exp\left[-B\left(\mathcal{E}(\frac{y - Vt}{S}, P) \right)^2 \right] + \exp\left[-B\left(1 - \mathcal{E}(\frac{y - Vt}{S}, P) \right)^2 \right] \tag{8}$$

[26] normalised by u_{ref}

[27] A wake defect of 30% means that u_w is equal to 30% of the reference axial velocity u_{ref}

with a spatial period determined by the stator-to-rotor blade ratio $K = \frac{N_s}{N_r}$ which will be taken as unity throughout this study [28] ; the function $\mathcal{E}(y, P)$ (Valkov 1992, 1995) is defined as

$$\mathcal{E}(y,K) = \begin{cases} y/K - E(y/K) & y \geq 0 \\ E(y/K) - y/K & y < 0 \end{cases} \quad (9)$$

and it describes the spatial periodicity

Table IV : Wakes Parameters for Numerical Simulations

Geometry	A	Z	B	δ	α_{in}
Eppler	0.15	0.27	100	0.32	33
E^3	0.225	0.32	100	0.35	44

B Control Volume Analysis

B.1 Mixing Loss

For a given flow configuration, the (time averaged) loss coefficient associated with mixing at a given x-location can be shown to be :

$$L_{mixing}(x) = \frac{\int_t^{t+T}\int_0^h (P_{tM}(x) - P_{ta}(x,y))u_a(x,y)dydt}{\frac{1}{2}u_{ref}^2(1+tan^2\theta_{ref})\int_0^h u_a(x,y)dy} \quad (10)$$

where subscript M refers to the mixed out quantities. The above integral can be rewritten as follows [29] :

$$L_{mixing}(x) = \frac{\int_t^{t+T}\int_0^h \left(\frac{1}{2}(u_M^2+v_M^2) - \frac{1}{2}(u_a(y)+v_a(y)^2)\right)dydt}{\frac{1}{2}u_{ref}^2(1+tan^2\theta_{ref})\int_0^h u(y)dy}$$

$$+\frac{\int_t^{t+T}\int_0^h (P_M(y) - P_a(y))u_a(y)dydt}{\frac{1}{2}u_{ref}^2(1+tan^2\theta_{ref})\int_0^h u(y)dydt} \quad (11)$$

The two parts correspond to a change in mass-averaged and time-averaged kinetic energy and pressure, respectively. Let us first calculate the part related to kinetic energy changes, which in turn can be written as :

$$Ł^K_{mixing}(x) = \frac{\int_t^{t+T}\int_0^h \left(\frac{1}{2}(u_M^2+v_M^2) - \frac{1}{2}(u_B^2(y)+v_B^2(y))\right)dydt}{\frac{1}{2}u_{ref}^2(1+tan^2\theta_{ref})\int_0^h u(y)dy}$$

$$-\frac{\int_t^{t+T}\int_0^h \left(\frac{1}{2}(u_a^2(y)+v_o^2(y)) - \frac{1}{2}(u_B^2(y)+v_B^2(y))\right)dydt}{\frac{1}{2}u_{ref}^2(\mathrm{I}+tan^2\theta_{ref})\int_0^h u(y)dy} \quad (12)$$

where the subscript B pertains to the steady (base) flow.

[28] In practice there will be less rotors than stators ($K > 1$). The analytical model based on the control volume approach of Appendix B and the kinematics of wakes given in Appendix C remain valid.

[29] The constant density ρ has been normalised so that it assumes a value of unity

The first term requires the knowledge of the axial and tangential mixed out velocities (at each time). Continuity conditions gives :

$$u_M = \frac{\int_0^h u_a(x,y)}{h} \quad (13)$$

while invoking the conservation of tangential momentum flux allows the tangential mixed out velocity to be expressed as :

$$v_M = \frac{\int_0^h u_a(x,y)v_a(x,y)}{hU_M} \quad (14)$$

The second part of Eq. (11) (related to the pressure) can also be rewritten as follows :

$$Ł^P_{mixing} = \frac{\int_t^{t+T}\int_0^h (P_M(y) - P_A(y))u_a(y)dydt}{\frac{1}{2}u_{ref}^2(1+tan^2\theta_{ref})\int_0^h u_a(y)dy}$$

$$+\frac{\int_t^{t+T}\int_0^h (P_A(y) - P(y))u(y)dydt}{\frac{1}{2}u_{ref}^2(1+tan^2\theta_{ref})\int_0^h u_a(y)dy} \quad (15)$$

where subscript A refers to the time and *area*-averaged pressure. In the first integral, the two terms are constant both in space and time. Upon using the axial momentum equation, their difference can be shown to be

$$\int_0^h (P_M(y) - P_A(y))dy =$$

$$\int_0^h (P_M(y) - P(y))dy = \rho\int_0^h (u_a^2(y) - u_M^2) \quad (16)$$

The second term in Eq. (15) has been shown to be negligible based on the computed results and will thus be assumed to be zero.

B.2 Isentropic pressure rise

The control volume analysis of section (2.3) shows that the difference in isentropic pressure rise between case a and b can be written :

$$\Delta P_{a-b} = \int_t^{t+T}\left\{\left(\int_{inlet}\frac{1}{2}U^2{}_a(y,t)dy - \int_{outlet}\frac{1}{2}U^2{}_a(y,t)dy\right)\right.$$

$$\left.-\left(\int_{inlet}\frac{1}{2}U^2{}_b(y,t)dy - \int_{outlet}\frac{1}{2}U^2{}_b(y,t)dy\right)\right\}dt \quad (17)$$

It has been found numerically that the outlet time-averaged tangential momentum flux is the same in case a and b, so that to a good degree of approxamation the velocities in case b can be replaced by the mixed out velocities obtained from case a; ΔP_{a-b} can thus be rewritten as :

$$\Delta P_{a-b} = \frac{1}{T}\int_t^{t+T}\left\{\left(\int_{inlet}\frac{1}{2}U_a^2(y,t)dy\right) - \frac{1}{2}U_m^2\right\}dydt$$

$$-\frac{1}{T}\int_t^{t+T}\left\{\left(\int_{outlet}\frac{1}{2}U_a^2(y,t)dy - \frac{1}{2}U_M^2(t)\right)\right\}dydt \quad (18)$$

C Kinematic Description of Flow

According to the integral forms given in Appendix B, only those aspects of the flow that affect the difference between the flow before and after mixing (both at the inlet and the outlet) are of interest. We shall therefore focus on these aspects of the flow which can significantly alter this difference. The unsteady flow is considered as the sum of a steady (base) flow and an unsteady disturbance flow. The (time averaged) mixed out conditions are obtained using Eq. (13) and (14). The velocity field can be written as:

$$\left\{ \begin{array}{c} u(y,t) \\ v(y,t) \end{array} \right\} = \left\{ \begin{array}{c} u_{ref} + u_p(y,t) \\ u_{ref} \tan\theta_{ref} + v_p(y,t) \end{array} \right\} \quad (19)$$

where u_p and v_p represent the axial and tangential velocity perturbation associated with the wakes (mixed out in case *b*). An analytical model for the velocity defect within the wakes at inlet and the outlet has to be developed.

C.1 Inlet

An analytical representation for the unsteady perturbation flow at the inlet is :

$$\left\{ \begin{array}{c} u_p(y,t) \\ v_p(y,t) \end{array} \right\} = \left\{ \begin{array}{c} -Zf(y,t)sin(\alpha_{inlet}) \\ Zf(y,t)cos(\alpha_{inlet}) \end{array} \right\} \quad (20)$$

where y varies from 0 to h and α_{inlet} is the angle between the wake and the vertical as shown in Fig. 9 :

$$\alpha_{inlet} = \tan^{-1}\left(\frac{u}{\frac{u}{\phi} - utan\theta}\right) \quad (21)$$

C.2 Outlet

To obtain a description of outlet perturbation flow, we must first determine the new wake angle α_{outlet} as well as the distance d_{adv} associated with the advection of the wake.

To derive an expression of α_{outlet}, we note that as the wake leaves the stator passage (Fig. 9), the lower portion of the wake (i.e. portion on the suction side of the blade) will be convected through a distance d before the upper portion (i.e. portion on the pressure side of the blade) reaches trailing edge. This distance d can also be equivalently given in terms of the traverse time $T_{SC} = T_{PA} + T_{PB} - T_{SB}$ (using the notations of Fig. 9).

The time T_{PA} shown in Fig. 9 is:

$$T_{PA} = \frac{d_{PA}}{u_{ref}} = \frac{h}{u_{ref}}\left(\tan\theta + \frac{1}{\tan\phi_{inlet}}\right)^{-1} \quad (22)$$

while time $(T_{PB} - T_{SB})$ can be estimated based on the times it would take for a fluid element to traverse the suction side and the pressure side. The portion of circulation associated with the

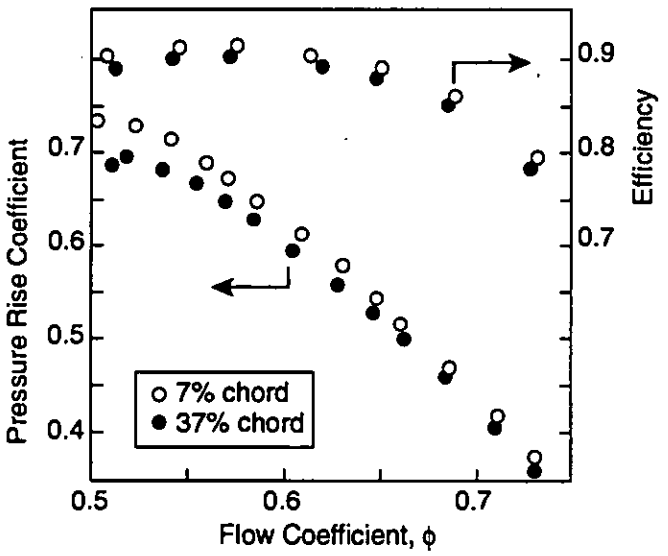

Figure 1: Compressor Performance at Two Different Axial Gaps (After Smith , 1970)

suction side and the pressure side are given respectively as Γ_{ss} ($\int_{ss} V_{ss} ds$) and Γ_{pp} ($\int_{ps} V_{ps} ds$); if c_{ss} and c_{ps} denote the extent of suction side and pressure side, then an average velocity (changes in blade velocity due to the passage of the wakes are neglected) can be defined for the suction side as $\bar{V}_{ss} = \frac{\Gamma_{ss}}{c_{ss}}$, and for the pressure side as $\bar{V}_{ps} = \frac{\Gamma_{ps}}{c_{ps}}$. From the above the traverse time $T_{SB} = \frac{c_{ss}}{\bar{V}_{ss}}$ and $T_{PB} = \frac{c_{ps}}{\bar{V}_{ps}}$ can be determined. The difference in traverse time between the pressure and the suction side can now be determined as:

$$T_{PB} - T_{SB} = \frac{c_{ps}^2\Gamma_{ss} - c_{ss}^2\Gamma_{ps}}{\Gamma_{ss}\Gamma_{ps}} \quad (23)$$

The wake angle α_{outlet} and the extent of the stretching s_{out} of the wake between the inlet and the outlet are given as :

$$\left\{ \begin{array}{l} \alpha_{outlet} = \tan^{-1}\frac{u_{ref}(T_{PA}+T_{PB}-T_{SB})}{h} \\ s_{out} = \sqrt{\frac{u_{ref}^2(T_{PA}+T_{PB}-T_{SB})^2+h^2}{d_{PA}^2\left(1+\frac{1}{\tan^2\phi_1}\right)}} \end{array} \right. \quad (24)$$

The wakes are asumed to be advected at a constant velocity

$$V_{adv} = \frac{Z}{4}\left(1 + \frac{1}{s_{out}}\right) \quad (25)$$

which is the average between that at the inlet and the outlet.

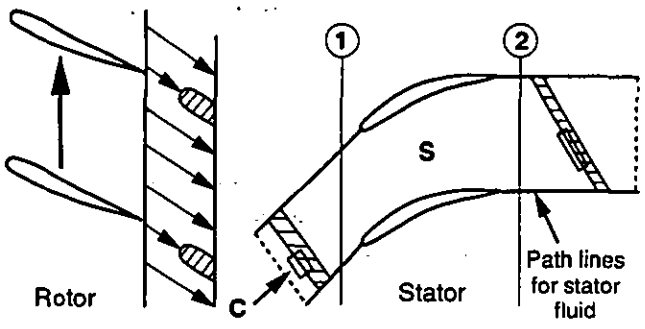

Figure 2: Overall Kinematics of Rotor-wakes-stator Interactions (After Smith, 1966)

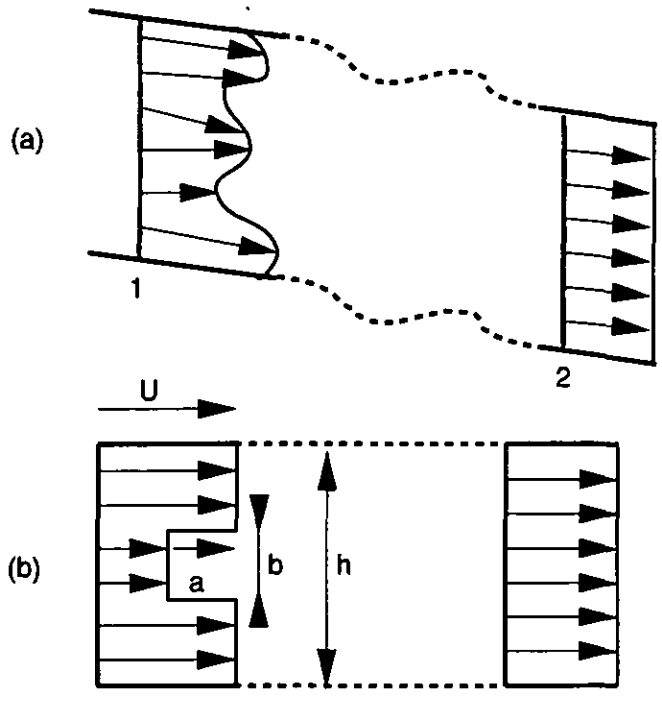

Figure 3: An Illustration of Mixing-out Flow Non-uniformity

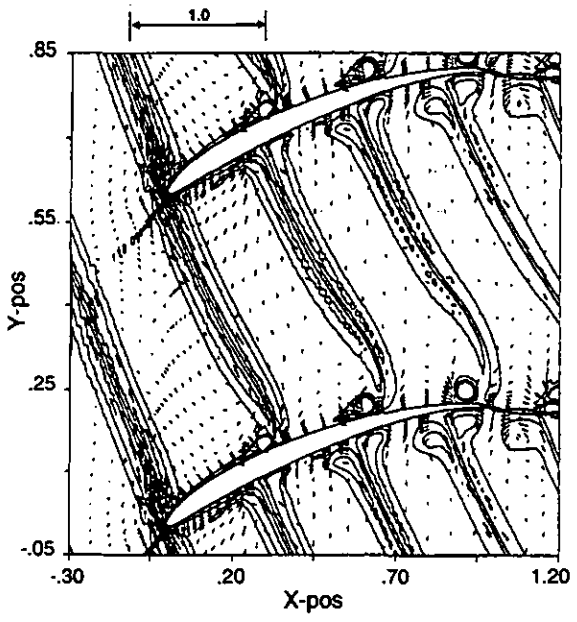

Figure 4: Disturbance Velocity and Vorticity Field Associated with Wakes Interacting with Stator Blades of Eppler Type; shown at Top of Figure is a Normalised Velocity Vector of Unity.

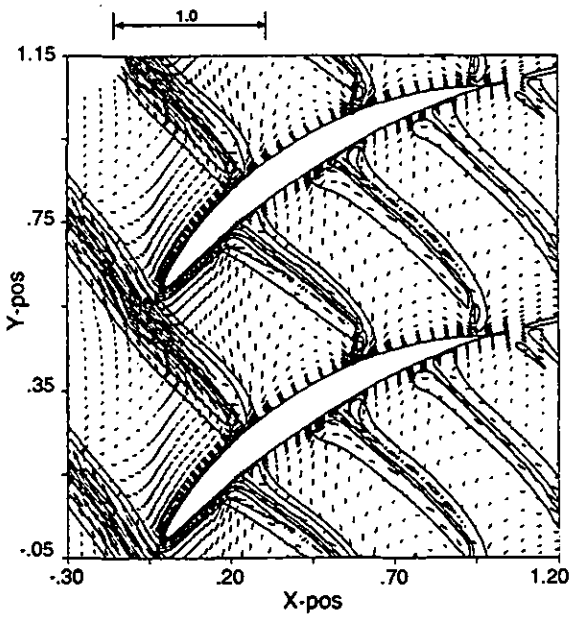

Figure 5: Disturbance Velocity and Vorticity Field Associated with Wakes Interacting with Stator Blades of E^3 Type; shown at Top of Figure is a Normalised Velocity Vector of Unity.

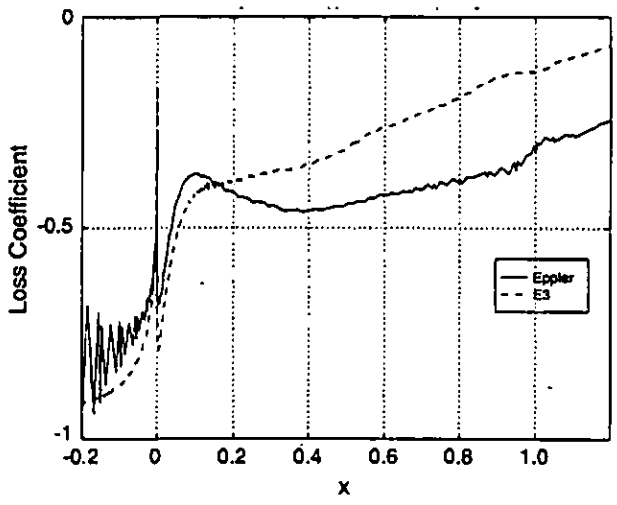

Figure 6: Axial Variation of Mixing Loss (expressed as percentage of inlet dynamic head; negative value implies a loss) for Rotor Wakes Interacting with Stator Blades of Eppler and E^3 Type

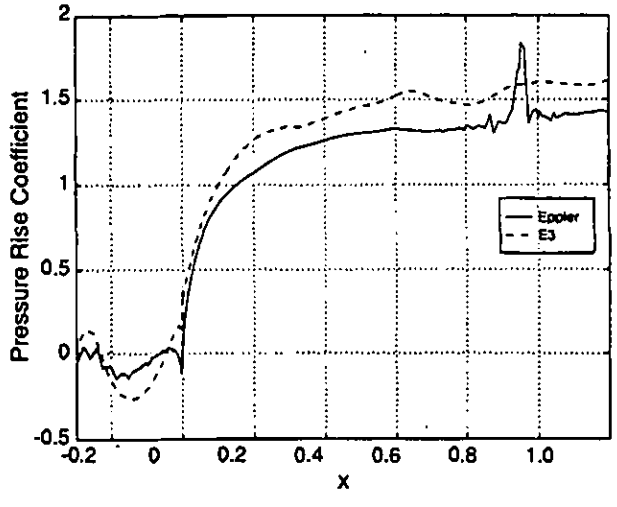

Figure 7: Axial Variation of Difference in Pressure Rise (expressed as percentage of inlet dynamic head) for Rotor Wakes Interacting with Stator Blades of Eppler and E^3 Type

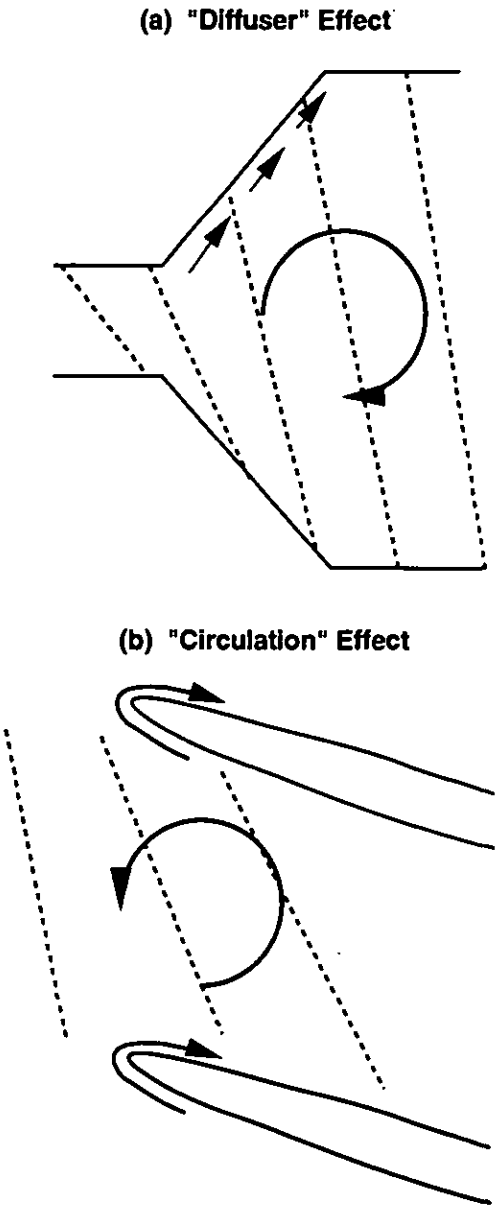

Figure 8: Turning of Wake as It Passes through the Stator Blade Passage

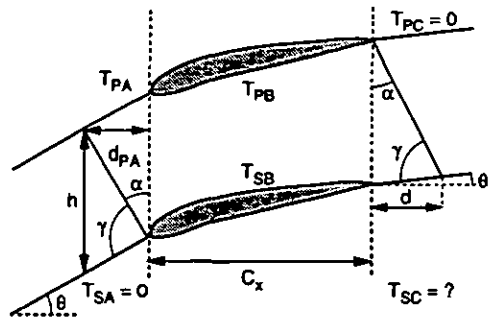

Figure 9: Notations Used in Analytical Model

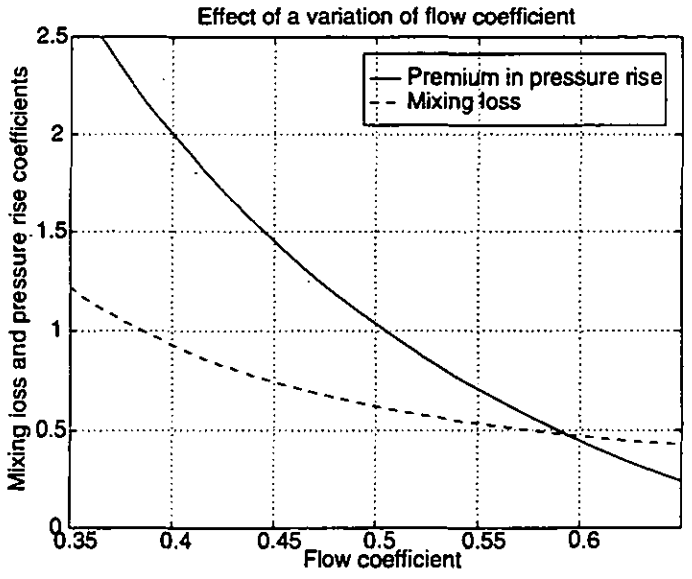

Figure 11: Effect of Flow Coefficient Variation on Mixing Loss and Difference in Pressure Rise (expressed as percentage of inlet dynamic head)

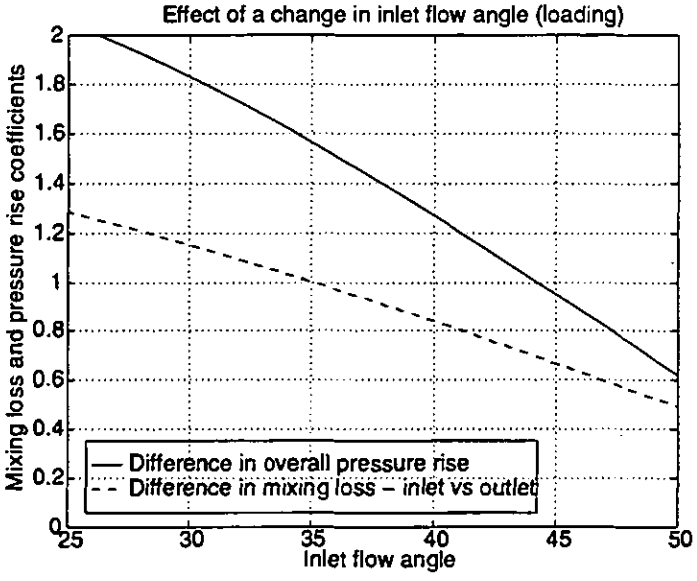

Figure 10: Effect of Inlet Flow Angle Variation on Mixing Loss and Difference in Pressure Rise (expressed as percentage of inlet dynamic head)

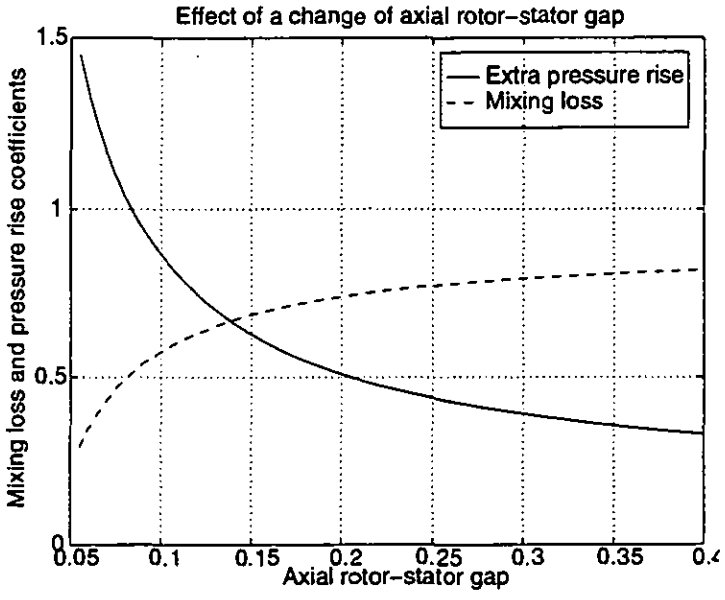

Figure 12: Effect of Axial Rotor-stator Gap Variation on Mixing Loss and Difference in Pressure Rise (expressed as percentage of inlet dynamic head)